© 2020. Published by The Company of Biologists Ltd | Development (2020) 147, dev185199. doi:10.1242/dev.185199

RESEARCH ARTICLE

Rnf220/Zc4h2-mediated monoubiquitylation of Phox2 is required for noradrenergic neuron development

Ning-Ning Song[1,*], Pengcheng Ma[2,*], Qiong Zhang[1,*], Lei Zhang[3], Huishan Wang[2,4], Longlong Zhang[2,4], Liang Zhu[2,4], Chun-Hui He[3], Bingyu Mao[2,5,‡] and Yu-Qiang Ding[1,3,‡]

ABSTRACT

Noradrenaline belongs to the monoamine system and is involved in cognition and emotional behaviors. Phox2a and Phox2b play essential but non-redundant roles during development of the locus coeruleus (LC), the main noradrenergic (NA) neuron center in the mammalian brain. The ubiquitin E3 ligase Rnf220 and its cofactor Zc4h2 participate in ventral neural tube patterning by modulating Shh/Gli signaling, and *ZC4H2* mutation is associated with intellectual disability, although the mechanisms for this remain poorly understood. Here, we report that Zc4h2 and Rnf220 are required for the development of central NA neurons in the mouse brain. Both *Zc4h2* and *Rnf220* are expressed in developing LC-NA neurons. Although properly initiated at E10.5, the expression of genes associated with LC-NA neurons is not maintained at the later embryonic stages in mice with a deficiency of either *Rnf220* or *Zc4h2*. In addition, we show that the Rnf220/Zc4h2 complex monoubiquitylates Phox2a/Phox2b, a process required for the full transcriptional activity of Phox2a/Phox2b. Our work reveals a role for Rnf220/Zc4h2 in regulating LC-NA neuron development, and this finding may be helpful for understanding the pathogenesis of *ZC4H2* mutation-associated intellectual disability.

KEY WORDS: Rnf220, Zc4h2, Noradrenergic neurons, Locus coeruleus, Phox2a, Phox2b, Monoubiquitylation, Mouse

INTRODUCTION

Noradrenergic (NA) neurons are located in both the central nervous system (CNS) and the peripheral nervous system. In the CNS, these neurons mainly reside in the brainstem and can be classified into six groups by their locations, including: the locus coeruleus (LC) group (A6), the subcoeruleus group and four other groups (A1, A2, A5 and A7) (Robertson et al., 2013). LC-NA neurons (NA neurons located in the LC) represent the vast majority of noradrenaline-releasing neurons in the CNS, with widespread projection in the brain. Dysfunction of the NA system is implicated in both psychiatric and neurodegenerative disorders, such as cognition decline, anxiety, depression, and Parkinson's and Alzheimer's diseases (Sara, 2009; Itoi and Sugimoto, 2010; Szot, 2012).

LC-NA neurons are generated from dorsal rhombomere 1 (r1) around embryonic day (E) 10.5 and migrate tangentially and ventrally to the dorsolateral pons at the late embryonic stages (Robertson et al., 2013). The genetic cascade controlling the development of LC-NA neurons has been extensively documented. FGF8 expressed in the mid-hindbrain border (isthmus), and BMPs and Wnts expressed in the roof plate, are essential for the specification of NA progenitors (Vogel-Hopker and Rohrer, 2002; Holm et al., 2006; Tilleman et al., 2010). Notch/Rbpj signaling in the ventricular zone is also involved, shown by findings that LC-NA neurons significantly increase in number when this signaling pathway is blocked (Shi et al., 2012). On the other hand, deletion of *Ascl1* (*Mash1*) leads to a failure of NA neuron generation (Hirsch et al., 1998). In addition, the roles of transcription factors expressed in postmitotic LC-NA neurons have also been revealed (Flames and Hobert, 2011). Among these factors, the homeodomain transcription factors Phox2a and Phox2b have attracted the most attention, because they are selectively expressed in postmitotic LC-NA neurons and directly control the expression of tyrosine hydroxylase (Th) and dopamine-β-hydroxylase (Dbh), two key enzymes that are responsible for noradrenaline biosynthesis. In the LC, Phox2a is activated first and is required for the expression of Phox2b (Morin et al., 1997; Pattyn et al., 1997). The expression of Phox2b is transient and downregulated at E13.5 in the LC (Pattyn et al., 2000), whereas ongoing expression of Phox2a is required for maintenance of NA differentiation. LC-NA neurons cannot be generated in mice with constitutive knockout (KO) of either *Phox2a* or *Phox2b* (Pattyn et al., 1997; Flames and Hobert, 2011). Deletion of *Phox2a* and *Phox2b* simultaneously at the adult stage also impairs the maintenance of LC-NA neurons (Coppola et al., 2010).

ZC4H2, an X-chromosome-linked intellectual disability (XLID) gene, encodes a C4H2 type zinc-finger nuclear factor, the mutation of which causes arthrogryposis multiplex congenita, intellectual disability and other defects (Hirata et al., 2013; May et al., 2015; Zanzottera et al., 2017). We previously reported that Zc4h2-mediated control of BMP/Smads signaling is required for *Xenopus* early neural development (Ma et al., 2017). Rnf220 is a RING finger domain ubiquitin E3 ligase that is responsible for the polyubiquitylation and degradation of Sin3B, a global regulator of gene transcription, which serves as an essential scaffold protein of the Sin3/HDAC corepressor complex (Kong et al., 2010), and involved in the regulation of canonical Wnt signaling through modulating USP7-mediated deubiquitylation of β-catenin (Ma et al., 2014). Recently, we reported that *Zc4h2* and *Rnf220* show similar expression patterns in the spinal tube and are required for ventral spinal tube patterning through modulation of Shh/Gli

[1]State Key Laboratory of Medical Neurobiology and MOE Frontiers Center for Brain Science, Institutes of Brain Science, Fudan University, Shanghai 200032, China. [2]State Key Laboratory of Genetic Resources and Evolution, Kunming Institute of Zoology, Chinese Academy of Sciences, Kunming 650223, China. [3]Key Laboratory of Arrhythmias, Ministry of Education of China, East Hospital, and Department of Anatomy and Neurobiology, Tongji University School of Medicine, Shanghai 200092, China. [4]Kunming College of Life Science, University of Chinese Academy of Sciences, Kunming 650203, China. [5]Center for Excellence in Animal Evolution and Genetics, Chinese Academy of Sciences, Kunming 650223, China.

*These authors contributed equally to this work

‡Authors for correspondence (dingyuqiang@vip.163.com; mao@mail.kiz.ac.cn)

N.-N.S., 0000-0001-5206-1911; P.M., 0000-0002-1067-8021; Q.Z., 0000-0001-7930-7643; L.Z., 0000-0001-7242-5292; B.M., 0000-0002-7993-3158; Y.-Q.D., 0000-0003-1202-4635

Received 1 October 2019; Accepted 11 February 2020

Development (2020) 147, dev185199. doi:10.1242/dev.185199

signaling in the mouse (Ma et al., 2019a; Ma et al., 2019b). Our and Kim's studies have shown that Zc4h2 interacts with Rnf220, and enhances the stability of Rnf220 both *in vitro* and *in vivo* (Kim et al., 2018; Ma et al., 2019a). However, the functions of *Zc4h2* and *Rnf220* in the development of the brain remain unknown.

In a microarray profiling analysis, we saw that the expression of the LC marker *Dbh* was greatly reduced in the *Rnf220* KO mouse brain (data to be published elsewhere), suggesting possible deficiency of LC-NA neurons in the absence of Rnf220. Here, we analyze in detail the roles of Zc4h2 and Rnf220 in the development of LC-NA neurons in the mouse. *Zc4h2* and *Rnf220* are both expressed in developing LC-NA neurons, and KO of either gene leads to a complete loss of expression of LC-NA neuron-associated genes at late embryonic stages, although the initiation of these genes are normal at the beginning of development. Furthermore, we provide evidence that the Zc4h2 and Rnf220 complex interacts with and monoubiquitylates Phox2a and Phox2b, promoting transactivation of Phox2a/Phox2b and expression of *Th* and *Dbh*, the hallmark of normal NA neuron differentiation.

RESULTS

Zc4h2 is required for LC-NA neuron development

The expression of Zc4h2 was examined in combination with molecular markers of NA neurons in mouse embryos at different embryonic stages. At E10.5, *Dbh* transcripts were observed in the dorsal r1, where LC-NA neurons are born (Hirsch et al., 1998), and these Dbh^+ cells also expressed Phox2a and Phox2b (Fig. 1A). No Zc4h2 immunoreactivity was detected at this stage (Fig. 1A). At E11.5, Zc4h2 expression was observed in the presumptive LC based on similar locations of $Zc4h2^+$ and Dbh^+ cells, shown by immunostaining of adjacent sections (Fig. S1A,B). In addition, BrdU labeling showed that Zc4h2 was expressed outside the $BrdU^+$ ventricular zone (Fig. S1C). At E12.5, Zc4h2 and Phox2a/Phox2b were expressed in Dbh^+ NA neurons (Fig. 1B), and some $Zc4h2^+$ cells without *Dbh* expression were located ventrolateral to NA neurons (Fig. 1B). At E16.5, Phox2a was expressed only in Th^+ neurons in the LC (Fig. 1C), and cells with only faint, if any, Phox2b immunoreactivity were located within the LC; in contrast, many cells with strong Phox2b immunoreactivity were located outside (dorsal to) the LC (Fig. 1C). At this stage, intense Zc4h2 signals were observed in the LC and Barrington's nucleus located ventromedial to the LC (Fig. 1C). Collectively, the findings indicated that Zc4h2 is expressed in developing LC-NA neurons.

The role of Zc4h2 in the development of LC-NA neurons were examined in *Zc4h2* KO embryos, in which the loss of *Zc4h2* was confirmed (Fig. 2A). At E10.5, the expression of *Dbh*, *Phox2a* and *Phox2b* appeared not to be changed in *Zc4h2* KO embryos compared with controls (Fig. 2C). At E12.5, however, *Dbh* expression was significantly reduced, and *Phox2a* expression was slightly reduced without obvious alterations of *Phox2b* expression in *Zc4h2* KO embryos relative to controls (Fig. 2D). The statistical data demonstrating the decrease of Dbh^+ neurons in *Zc4h2* KO mice is shown in Fig. 2B. At E16.5, neither *Dbh* nor *Phox2a*/*Phox2b* expression was observed in *Zc4h2* KO embryos (Fig. 2E). Because the *Zc4h2* gene is located on the X chromosome, the female *Zc4h2* heterozygote is a chimera with both wild-type cells and *Zc4h2* mutant cells because of random X inactivation, as reported previously (Ma et al., 2019a). Indeed, the number of $Zc4h2^+$ cells

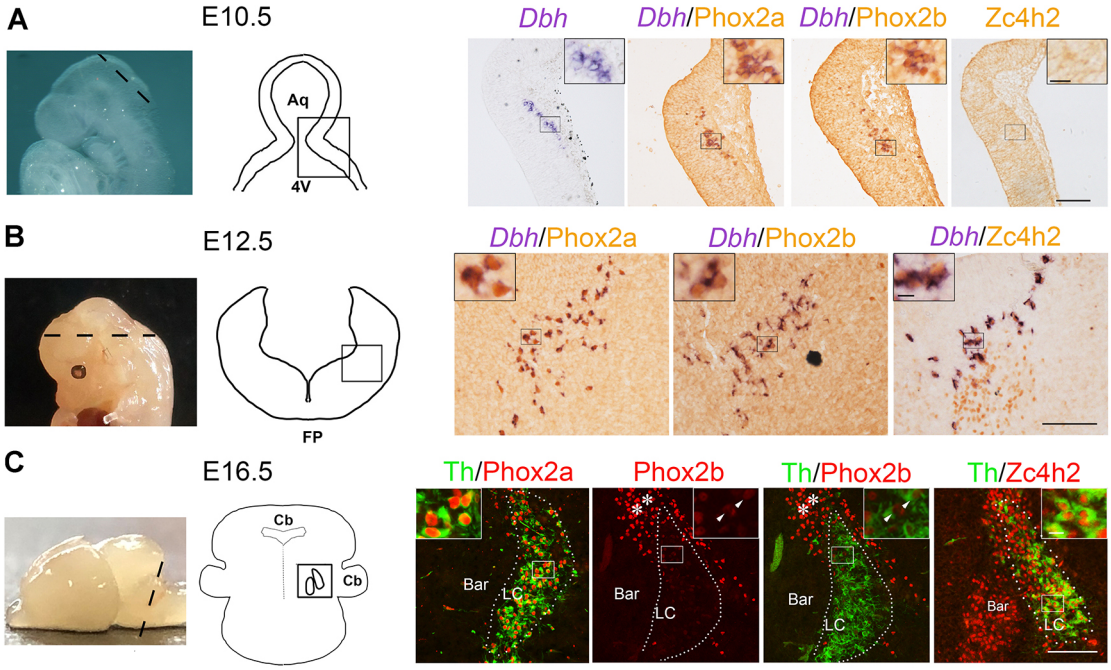

Fig. 1. Expression of Zc4h2 in developing LC-NA neurons. (A) Left two panels: whole embryo view and diagram showing level of section (dashed line) in E10.5 embryos. Right four panels: *in situ* hybridization of *Dbh*, double labeling of *Dbh* mRNA with Phox2a/Phox2b proteins, and immunostaining of Zc4h2 are shown in the representative sections. (B) Left two panels: whole embryo view and diagram showing level of section (dashed line) in E12.5 embryos. Right three panels: double labeling of *Dbh* mRNA with Phox2a/Phox2b/Zc4h2 proteins are shown in the representative sections. (C) Left two panels: whole embryo view and diagram showing level of section (dashed line) in E16.5 embryos. Right four panels: double immunostaining of Th with Phox2a, immunostaining of Phox2b, double immunostaining of Phox2b with Th, and double immunostaining of Zc4h2 with Th are shown in the representative sections. Zc4h2 is also observed in Barrington's nucleus (Bar) located ventromedially to the locus coeruleus (LC). Arrowheads indicate double labeling of weak Phox2b and Th. Asterisks indicate the region with high Phox2b expression outside the LC. Dotted lines demarcate the LC. 4V, fourth ventricle; Aq, aqueduct; Cb, cerebellum; FP, floor plate. Scale bars: 100 µm; 20 µm in inset.

Development (2020) 147, dev185199. doi:10.1242/dev.185199

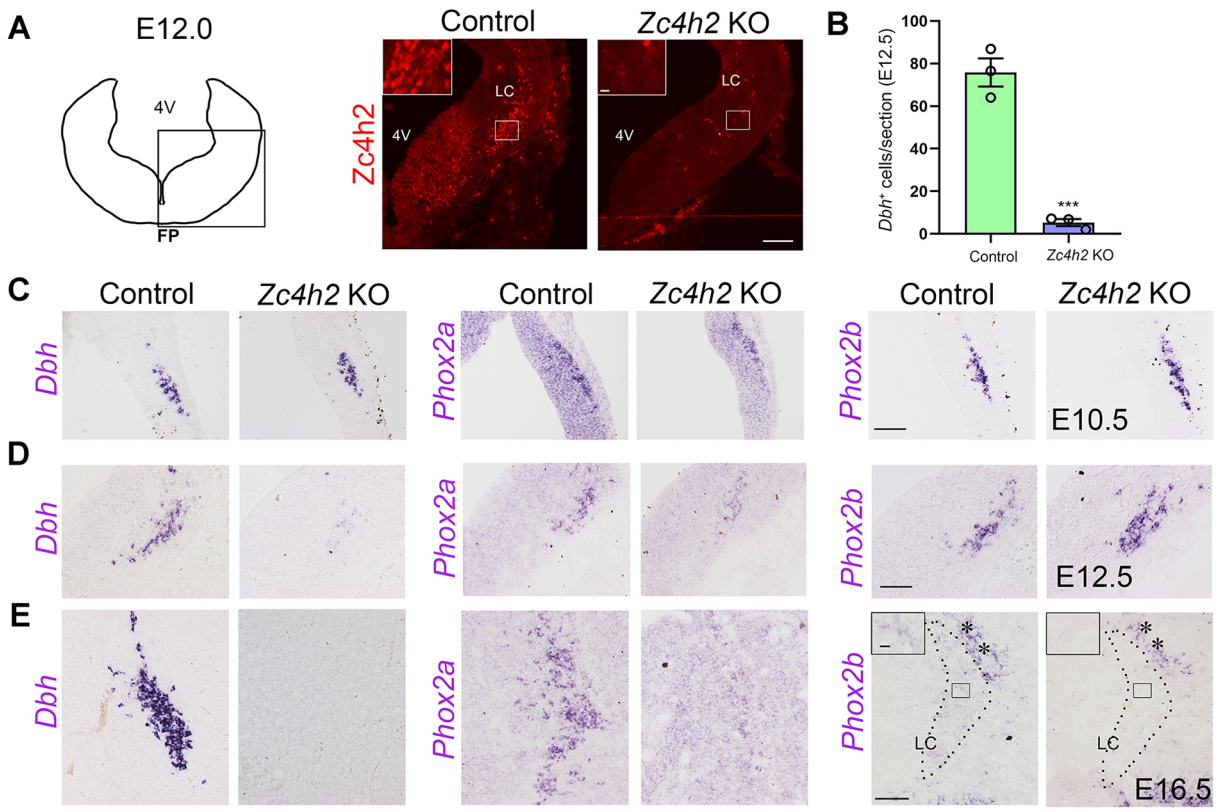

Fig. 2. The defective development of LC-NA neurons in *Zc4h2* KO embryos. (A) Immunostaining of Zc4h2 in controls and *Zc4h2* KO embryos at E12.0. (B) The *Dbh*$^+$ cell numbers in presumptive LC of control and *Zc4h2* KO embryos. Data are mean±s.e.m.; *n*=3; ***P=0.0006 (independent-samples *t*-test). (C-E) The distribution of *Dbh Phox2a* and *Phox2b* mRNA in the representative sections of controls and *Zc4h2* KO embryos at E10.5 (C), E12.5 (D) and E16.5 (E). Asterisks in E indicate the region with *Phox2b* expression outside the LC. Dotted lines demarcate the LC. 4V, fourth ventricle; FP, floor plate; LC, locus coeruleus. Scale bars: 100 µm; 20 µm in inset in A; 10 µm in inset in E.

appeared to be reduced in the presumptive rostral pons containing LC-NA neurons in female heterozygotes relative to female controls at E12.5 (Fig. S2A-C). Importantly, *Dbh* expression was also reduced in the heterozygotes at E12.5 (Fig. S2D). Thus, our data from both mutant and female heterozygotes indicate that Zc4h2 is required for the normal development of LC-NA neurons.

Rnf220 is also required for LC-NA neuron development

Next, we examined the expression of *Rnf220* in developing LC-NA neurons. *Rnf220* mRNA was detected in the dorsal r1 at E10.5, and its distribution overlapped with that of *Dbh* transcripts at E10.5 and E12.5 (Fig. 3A,B). At E16.5, *Rnf220* mRNA was strongly expressed in both the LC and Barrington's nucleus, and this pattern was almost identical to that of Zc4h2 in the dorsolateral pons (Fig. 3C). Double immunostaining of Zc4h2 protein and *Rnf220* mRNA confirmed the co-localization of the two genes in LC-NA neurons at E11.5 (Fig. S1D).

Successful deletion of the *Rnf220* gene was confirmed by *in situ* hybridization with probes specifically targeting exon 2 (*Rnf220* E2) at E10.5 (Fig. 3D). The expression of *Dbh*, *Phox2a* and *Phox2b* was similar in *Rnf220* KO and control embryos at E10.5 (Fig. 3E). At E12.5, however, the expression of *Dbh* and *Phox2a* was reduced, although the expression of *Phox2b* was not obviously changed in *Rnf220* KO embryos compared with controls (Fig. 3F). The statistical data demonstrating the decrease of *Dbh*$^+$ neurons in *Rnf220* KO mice is shown in Fig. 3G. At E16.5, the expression of *Dbh*, *Phox2a* and *Phox2b* was hardly detected in the LC region in *Rnf220* KO embryos (Fig. 3H). The expression of other genes associated with LC-NA neurons, including aromatic amino acid decarboxylase (*Aadc*; also known as *Ddc*), monoamine oxidase A (*MaoA*), norepinephrine transporter (*Net*; *Slc6a2*) and *Th*, was also examined, and their expression was completely lost in both *Rnf220* and *Zc4h2* KO embryos at this stage (Fig. 4A-C). As mentioned above, *Zc4h2* and *Rnf220* were also expressed in Barrington's nucleus. The expression of corticotropin-releasing factor (*Crf*; *Crh*), a marker for Barrington's nucleus (Flames and Hobert, 2011), did not significantly differ in either *Rnf220* KO or *Zc4h2* KO embryos relative to controls (Fig. 4D). Meanwhile, the expression of peripherin (*Peri*; *Prph*), which labels mesencephalic trigeminal nucleus (Me5) neurons located dorsolateral to LC neurons (Barclay et al., 2007), was not changed in *Rnf220* KO mice (Fig. 4C). In addition, no expression of *Rnf220* was found in the sympathetic ganglion, in which peripheral NA neurons are located, and peripheral NA neurons shown by Th immunostaining were not affected in *Rnf220* or *Zc4h2* KO embryos (Fig. S3A,B).

Taken together, these results indicate that defective development of LC-NA neurons occurs in *Rnf220* and *Zc4h2* KO embryos, suggesting that they may closely coordinate to regulate NA neuron development.

The Rnf220/Zc4h2 complex interacts with and monoubiquitylates Phox2a/Phox2b

Using co-immunoprecipitation (co-IP) assays, we tested whether Rnf220 or Zc4h2 interacts with factors involved in LC-NA neuron development, including Phox2a, Phox2b, Th and Dbh. When expressed alone, Zc4h2, but not Rnf220, pulled down Phox2a and Phox2b (Fig. S4A). When Rnf220 and Zc4h2 were co-expressed,

Development (2020) 147, dev185199. doi:10.1242/dev.185199

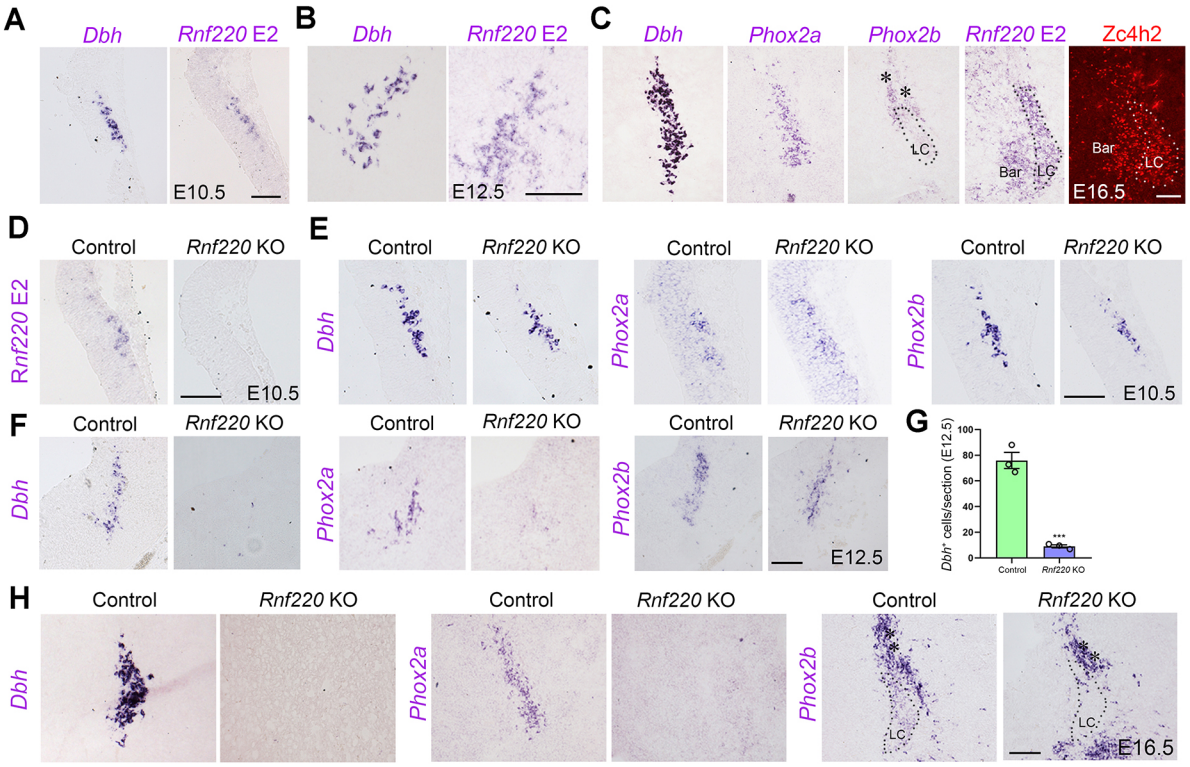

Fig. 3. *Rnf220* expression in presumptive LC and defective development of LC-NA neurons in *Rnf220* KO embryos. (A,B) The distributions of *Dbh* and *Rnf220* mRNA at E10.5 (A) and E12.5 (B). (C) The distributions of *Dbh*/*Phox2a*/*Phox2b*/*Rnf220* mRNA and Zc4h2 immunoreactivity at E16.5. Both *Rnf220* and Zc4h2 are also present in Barrington's nucleus (Bar) located ventromedially to LC. (D) The absence of *Rnf220* in *Rnf220* KO at E10.5 compared with age-matched controls. (E) The expression of *Dbh*, *Phox2a* and *Phox2b* in presumptive LC of controls and *Rnf220* KO embryos at E10.5. (F) The expression of *Dbh*, *Phox2a* and *Phox2b* in presumptive LC of controls and *Rnf220* KO embryos at E12.5. (G) The *Dbh*$^+$ cell numbers in presumptive LC of control and *Rnf220* KO embryos. Data are mean±s.e.m.; n=3; ***P=0.0004 (independent-samples t-test). (H) The expression of *Dbh*, *Phox2a* and *Phox2b* in presumptive LC of controls and *Rnf220* KO embryos E16.5. Asterisks in C and H indicate the region with high *Phox2b* expression outside the LC at E16.5. Bar, Barrington's nucleus; LC, locus coeruleus. Dotted lines demarcate the LC. Scale bars: 100 µm.

Rnf220 could also immunoprecipitate Phox2a and Phox2b in HEK293 cells (Fig. 5A), suggesting the formation of a ternary complex. Interestingly, an additional band was observed above the normal Phox2a and Phox2b band when Rnf220 and Zc4h2 were co-expressed (Fig. 5A,B, Fig. S4A,B and Fig. S5B), suggesting covalent modification of the proteins.

As Rnf220 is a ubiquitin E3 ligase, we then tested whether Rnf220/Zc4h2 ubiquitylates Phox2a and Phox2b. First, when the E3 ligase-dead W539R mutant was co-expressed with Zc4h2, the additional band of Phox2a or Phox2b was no longer observed (Fig. 5C and Fig. S4C), suggesting that the modification is dependent upon E3 ligase activity. In addition, we also carried out *in vivo* ubiquitylation assays using HA-tagged ubiquitin in HEK293 cells and found that the modification induced by wild-type Rnf220/Zc4h2 complex was monoubiquitylation (Fig. 5D and Fig. S4D). To identify the lysine residue ubiquitylated by Rnf220, we next mutated all the lysine residues one by one in both Phox2a and Phox2b, and examined the protein band patterns in the presence of Zc4h2 and Rnf220 (Fig. 5E and Fig. S4E). The results showed that K178 in Phox2a and K185 in Phox2b are the lysines that are monoubiquitylated by the Rnf220/Zc4h2 complex, because the mutations of these lysines (Phox2a K178R and Phox2b K185R) totally abolished the specific modified protein bands (Fig. 5F and Fig. S4F).

We also tested whether endogenous Phox2a/Phox2b is monoubiquitylated by Rnf220/Zc4h2 in the catecholaminergic mouse cell line CATH.a. Phox2a and Phox2b antibodies detected two main bands in CATH.a cell lysates. When *Rnf220* and *Zc4h2* were both knocked down by small interfering (si)RNAs, the intensities of the upper bands decreased (Fig. 5G), suggesting that Rnf220/Zc4h2 monoubiquitylates Phox2a/Phox2b *in vivo*. The knockdown efficiency of the siRNAs for *Zc4h2* and *Rnf220* was verified by real-time RT-PCR and western blot analysis (Fig. S5K,L and data not shown). Finally, we examined endogenous Phox2a and Phox2b for potential monoubiquitylation in E18.5 mid-hindbrain tissues from *Rnf220* and *Zc4h2* KO embryos. Indeed, specific upper bands for Phox2a and Phox2b were observed in hindbrain lysates from control embryos, but the intensities of these bands were dramatically reduced in both *Rnf220* KO and *Zc4h2* KO embryos (Fig. 5H,I). Together, the above data strongly suggest that Phox2a and Phox2b can be monoubiquitylated by the Zc4h2/Rnf220 complex. Interestingly, for Phox2a, the modified upper band appeared to be a doublet in both CATH.a cells and brain lysates, suggesting the presence of an additional modification or isoform of Phox2a *in vivo*.

Rnf220/Zc4h2-mediated monoubiquitylation of Phox2a/Phox2b favors Phox2a/Phox2b DNA-binding ability and transactivity

To explore the functional consequences of Phox2a and Phox2b monoubiquitylation by the Rnf220/Zc4h2 complex, we first examined the DNA-binding ability of Phox2a/2b through electrophoretic mobility shift assay (EMSA) gel shift assays. We found that Phox2a and Phox2b proteins from HEK293 cells with

Development (2020) 147, dev185199. doi:10.1242/dev.185199

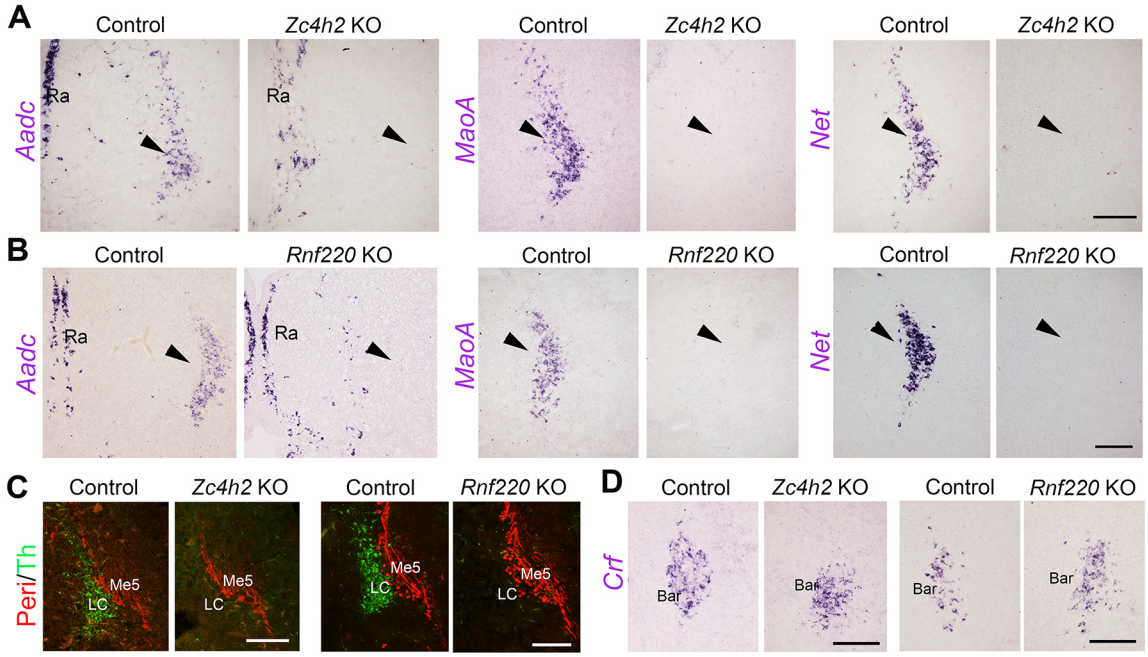

Fig. 4. Genes associated with LC-NA neurons are lost and *Crf* in Barrington's nucleus is not affected at E16.5 in *Zc4h2* and *Rnf220* KO embryos. (A) The distribution of *Aadc*, *MaoA* and *Net* transcripts are observed in LC of control but not *Zc4h2* KO embryos. (B) The distribution of *Aadc*, *MaoA* and *Net* transcripts are observed in LC of control but not *Rnf220* KO embryos. Arrowheads indicate the location of LC. (C) Double immunostaining of Th (green) and peripherin (Peri, red) shows the loss of Th expression in LC, which is located medially to Peri^{+} mesencephalic trigeminal nucleus (Me5), in *Zc4h2*/*Rnf220* KO embryos compared with controls. (D) The distribution of *Crf* mRNA in Barrington's nucleus (Bar), which is located ventromedially to LC, is maintained in both *Rnf220* and *Zc4h2* KO embryos. Ra, raphe nucleus; LC, locus coeruleus. Scale bars: 100 µm.

co-expression of the wild-type Rnf220/Zc4h2 complex showed enhanced DNA-binding ability compared with those from HEK293 cells with co-expression of ligase dead mutant Rnf220/Zc4h2 complex or control plasmids (Fig. 6A and Fig. S5A-C). Note that wild-type Phox2a and Phox2b and their KR mutants showed similar DNA-binding abilities (Fig. S5A,B), and Rnf220/Zc4h2 co-expression did not affect the DNA-binding ability of the two KR mutants (Fig. S5D,E). To examine the transcriptional activity of Phox2a and Phox2b, we conducted a human *DBH* promoter-driven reporter assay. It showed that the transactivity towards the expression of luciferase reporter was enhanced by wild-type Phox2a and Phox2b but not their KR mutants (Fig. 6B and Fig. S5F). We also examined the transcriptional activity of Phox2a and Phox2b by measuring *Th* and *DBH* expression levels in CATH.a cells. Co-expression of Zc4h2 and Rnf220 enhanced Phox2a and Phox2b transactivity towards *Th* and *DBH* expression, whereas Rnf220 alone or co-expression of Zc4h2 and the Rnf220 ligase mutant did not do so in CATH.a cells (Fig. 6C,D and Fig. S5G,H). The Phox2a K178R and Phox2b K185R mutants, which cannot be ubiquitylated by Rnf220/Zc4h2, exhibited reduced ability to activate *Th* and *Dbh* expression, and no enhancement was observed when Rnf220 and Zc4h2 were co-expressed (Fig. 6E,F and Fig. S5I,J). Furthermore, the expression levels of *Th* and *Dbh* were decreased when *Zc4h2* and *Rnf220* were both knocked down in CATH.a cells, but were not significantly changed in the case of single knockdown of *Zc4h2* or *Rnf220* (Fig. 6G,H), suggesting the possibility that the residual Zc4h2/Rnf220 complex still functions in the monoubiquitylation of Phox2a/Phox2b. Finally, we used *in ovo* electroporation assays in chick embryos to examine the effect of Rnf220-mediated monoubiquitylation on Phox2 proteins. We first confirmed the expression of overexpressed genes by *in situ* hybridization (*Phox2a*, *Phox2b* and *Rnf220*) and immunohistochemistry (Zc4h2) in the chick neural tube (Fig. S6). Co-expression of wild-type Phox2a/2b with the Rnf220/Zc4h2 complex induced strongly ectopic expression of *Dbh* in the chick neural tube, whereas ectopic *Dbh* expression induced by co-expression of the Phox2a/2b KR mutant with the Rnf220/Zc4h2 complex was less and weaker (Fig. 6I), supporting an *in vivo* role of Rnf220/Zc4h2 in the regulation of Phox2 transactivity. In addition, the ectopic expression of *Dbh* was weakly induced in the chick neural tube with overexpression of wild-type Phox2a/2b or their KR mutants but hardly detected in the tube with overexpression of the Rnf220/Zc4h2 complex alone (Fig. S5M). Taken together, these data suggest that Zc4h2/Rnf220-mediated monoubiquitylation of Phox2a and Phox2b favors transactivation of *Th* and *Dbh* expression by Phox2a and Phox2b (Fig. 6J).

DISCUSSION

Following up on our previous studies, we report that Rnf220 and Zc4h2 are required for the development of LC-NA neurons in the mouse brain. Through a mechanistic study, we demonstrated that the Rnf220/Zc4h2 complex monoubiquitylates Phox2a/Phox2b, which is required for the full transcriptional activity of Phox2a/Phox2b. In the absence of either Rnf220 or Zc4h2, the levels of monoubiquitylated Phox2a and Phox2b are reduced, which impairs the differentiation process of LC-NA neurons during embryonic development.

Both Zc4h2 and Rnf220 have similar expression profiles in differentiating LC-NA neurons. Zc4h2 directly binds to Phox2a/Phox2b and is necessary for the monoubiquitylation of Phox2a/Phox2b induced by Rnf220. The initiation of Phox2a, Phox2b and Rnf220 expression in presumptive LC-NA neurons occurs at E10.5, before the initiation of Zc4h2 expression. Thus, the post-translational modification of Phox2a/Phox2b by the Zc4h2/Rnf220

Development (2020) 147, dev185199. doi:10.1242/dev.185199

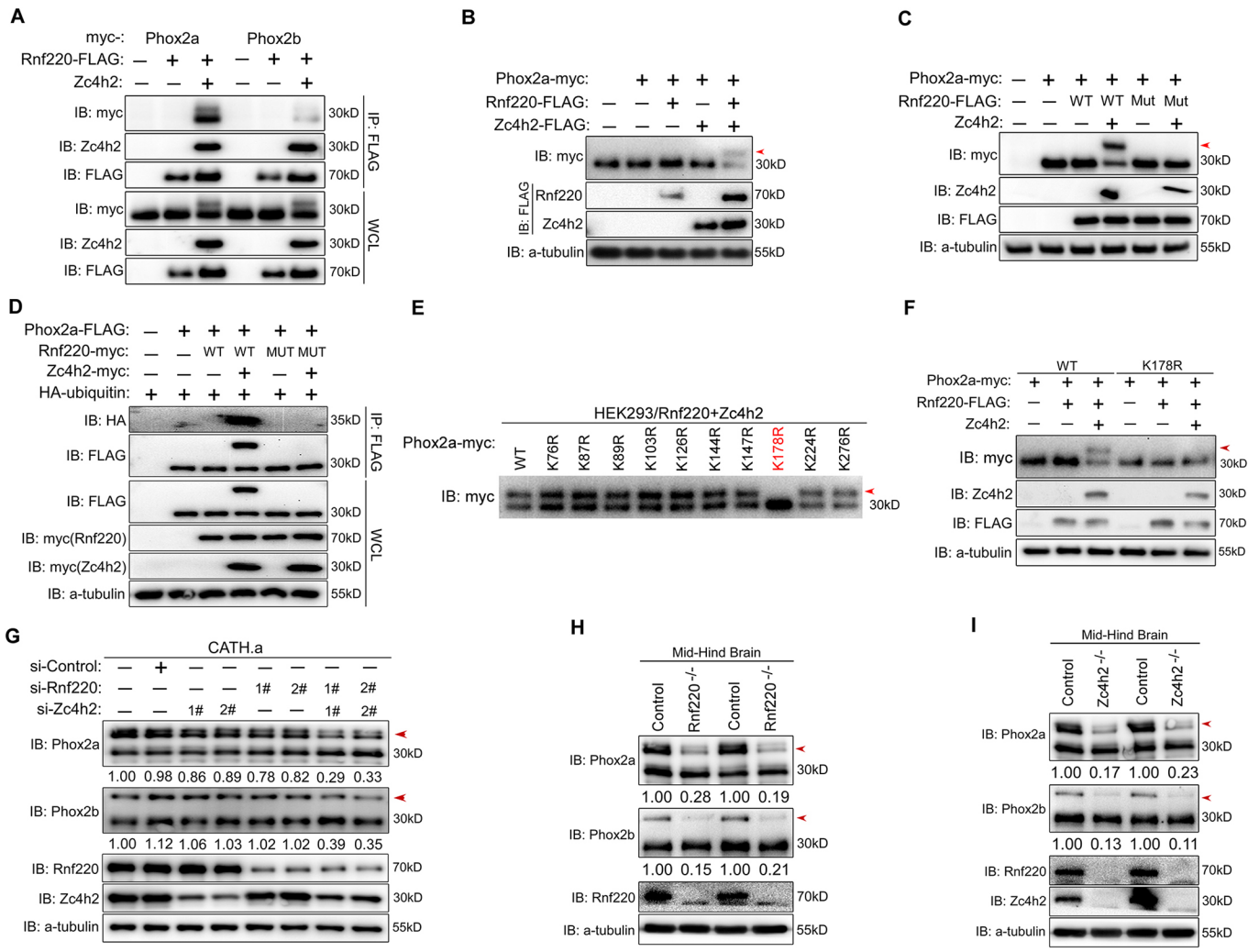

Fig. 5. Rnf220/Zc4h2 complex interacts with and monoubiquitylates Phox2. (A) Co-IP assays show the interaction between Phox2a/2b and the Rnf220/Zc4h2 complex. Phox2a and Phox2b are immunoprecipitated by Rnf220 only in the presence of Zc4h2 in HEK293 cells. The indicated plasmid combinations were transfected into HEK293 cells and cells were harvested at 48 h post transfection for IP analysis. The whole cell lysate and IP samples were analyzed by western blot. (B) Western blot data show that a covalent modification band (red arrowhead) of Phox2a was observed only when Rnf220 is co-expressed with Zc4h2 in HEK293 cells. (C) Western blot data show the presence of the covalent modification band (red arrowhead) of Phox2a when Zc4h2 was co-expressed with Rnf220 wild type or its ligase dead mutant in HEK293 cells. (D) *In vivo* ubiquitylation assays in HEK293 cells show that the covalent modification band of Phox2a mediated by Rnf220/Zc4h2 is monoubiquitylation. (E) Western blot results show the protein band pattern of Phox2a when the indicated lysines were mutated at the presence of Rnf220 and Zc4h2. (F) The Phox2a protein monoubiquitylation modification (red arrowhead) induced by the Rnf220/Zc4h2 complex is abolished when their indicated lysines are mutated in HEK293 cells. (G) Western blot data show the changes of endogenous Phox2a/Phox2b protein band pattern and their monoubiquitylation levels (red arrowheads) in CATH.a cells when *Rnf220* and/or *Zc4h2* are knocked down by siRNAs. (H,I) Western blot data show endogenous Phox2a/Phox2b protein band pattern and their monoubiquitylation levels (red arrowheads) in mid-hindbrain tissues of E18.5 controls and *Rnf220* KO (H) and *Zc4h2* KO (I) embryos. The relative levels of the monoubiquitylated Phox2a and Phox2b in G-I normalized to α-tubulin are shown below the indicated panels, respectively. All the related experiments were carried out three times. WCL, whole cell lysate; IP, immunoprecipitation.

complex does not occur, and the differentiation of LC-NA neurons is unaffected in *Zc4h2* and *Rnf220* KO embryos at E10.5. As development progresses, *Zc4h2* expression is initiated in differentiating LC-NA neurons at E11.5, and modification of Phox2a/Phox2b by the Rnf220/Zc4h2 complex may begin in order to enable proper differentiation of LC-NA neurons. As Phox2a and Phox2b directly regulate the expression of *Dbh* and *Th* (Fig. 6 and Fig. S5) and auto-regulate themselves (Rychlik et al., 2005), deficient modification of Phox2a/Phox2b protein by the Zc4h2/Rnf220 complex may account for the downregulated expression of *Phox2a* and *Dbh* at E12.5 and the total loss of the expression of LC-NA neuron-associated genes in *Zc4h2* and *Rnf220* KO embryos at E16.5. However, the terminal fate of LC-NA neurons is still unknown because of the lack of a specific marker to label the mutant LC-NA neurons in *Zc4h2* and *Rnf220* KO embryos. In addition to Phox2a and Phox2b, the transcription factors Tlx3 (Rnx) and AP-2β (Tfap2b) are also involved in the differentiation or survival of LC-NA neurons (Qian et al., 2001; Hong et al., 2008; Flames and Hobert, 2011). It is unknown whether these factors are also regulated by the Rnf220/Zc4h2 complex. Interestingly, peripheral NA neurons were not affected in *Rnf220* or *Zc4h2* KO mice. Central and peripheral NA neurons share similar regulatory signals but differ in other pathways (Brunet and Pattyn, 2002; Howard, 2005; Flames and Hobert, 2011). For example, Gata3 is expressed in sympathetic NA neurons and is

Development (2020) 147, dev185199. doi:10.1242/dev.185199

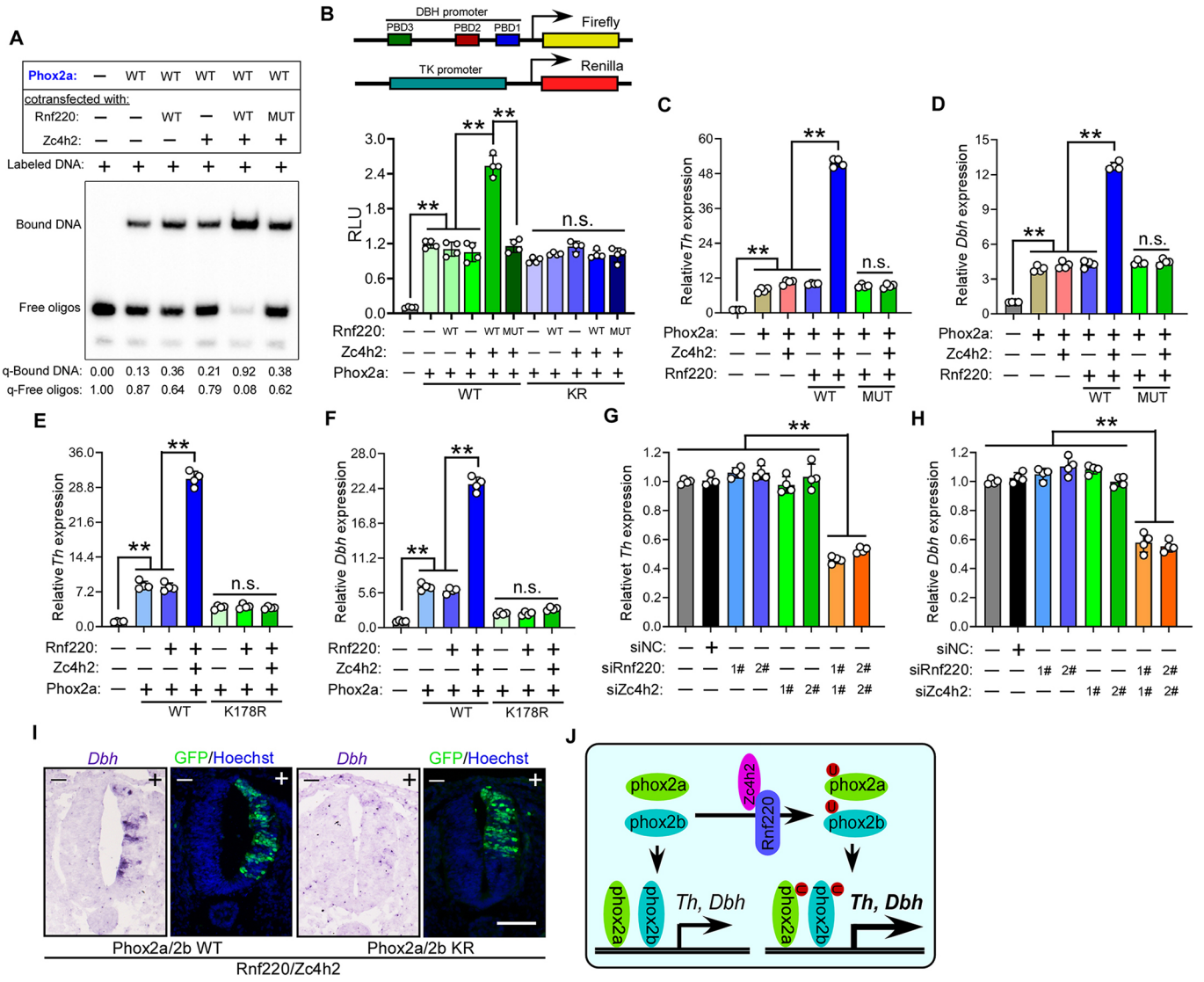

Fig. 6. Monoubiquitylation of Phox2a/2b by the Rnf220/Zc4h2 complex enhances their DNA-binding abilities and transactivities. (A) Gel shift assays show that Phox2a protein from HEK293 cells overexpressing wild-type Rnf220/Zc4h2 displays enhanced DNA binding abilities. (B) Reporter assays show that Phox2a monoubiquitylation mediated by Rnf220/Zc4h2 displays enhanced transactivities. The upper panel shows the illustration of the reporters used in these assays. PGL3 basic construct with the insertion of the three Phox2 binding sites of human *DBH* promoter (PBD1, PBD2 and PBD3) was used as the reporter constructs and the TK-*Renilla* was used as an internal control. (C,D) Real-time PCR assays show the relative expression levels of *Th* (C) and *Dbh* (D) when the indicated combination of *Phox2a*, *Zc4h2* and/or *Rnf220* plasmids are co-expressed in CATH.a cells. (E,F) Real-time PCR assays show the relative expression levels of *Th* (E) and *Dbh* (F) when the indicated combination of wild-type *Phox2a* or its K178R mutant, *Zc4h2* and/or *Rnf220* plasmids are co-expressed in CATH.a cells. (G,H) Real-time PCR assays show the relative expression levels of *Th* (G) and *Dbh* (H) when *Rnf220* and/or *Zc4h2* are knocked down by siRNA in CATH.a cells. The indicated plasmids or siRNA combinations were transfected into CATH.a cells and cells were harvested at 72 h post-transfection. Total RNA was extracted and assessed using real-time RT-PCR assays. (I) Ectopic expression of *Dbh* is induced in the chick neural tube by co-expression of wild-type Phox2a/2b with the Rnf220/Zc4h2 complex. It is much weaker in the tube after the co-expression of Phox2a/2b KR mutants with the Rnf220/Zc4h2 complex. Scale bar: 100 µm. (J) Working model of the Rnf220/Zc4h2 complex, which monoubiquitylates Phox2a/2b, enhancing their transactivities towards *Th* and *Dbh* expression during the development of LC-NA neurons in the mouse brain. Data are mean±s.e.m. $^{**}P<0.01$, one-way ANOVA evaluations with posthoc Student–Newman–Keuls test. n.s., not significant.

required for their differentiation and maintenance in embryos and adult mice (Lim et al., 2000; Tsarovina et al., 2010). However, no expression of Gata3 is found in LC-NA neurons (Zhao et al., 2008), and Rnf220 is absent in the sympathetic ganglia. Such differences might account for the different requirements of Phox2a/Phox2b modification by Rnf220/Zc4h2 for the differentiation of NA neurons in the sympathetic ganglia and LC.

Rnf220 has been reported to function through diverse mechanisms in different scenarios; for example, it promotes proteasomal degradation of Sin3B via canonical polyubiquitylation, stabilizes β-catenin through USP7-mediated deubiquitylation in cultured mammalian cells, and changes Glis subcellular location through K63-linked polyubiquitylation during ventral spinal tube patterning (Kong et al., 2010; Ma et al., 2014; Ma et al., 2019b). Zc4h2 is a close partner and stabilizer of Rnf220 (Kim et al., 2018; Ma et al., 2019a). Monoubiquitylation of proteins can alter their activity, structure or localization (Hicke, 2001; Haglund et al., 2003). Although the underlying mechanism remains to be investigated, the present

Development (2020) 147, dev185199. doi:10.1242/dev.185199

results emphasize a pivotal role of Zc4h2/Rnf220-mediated Phox2 monoubiquitylation in ensuring full transactivation of Th and Dbh expression, whereby Rnf220/Zc4h2 regulates the development of LC-NA neurons. It is possible that the monoubiquitylation of Phox2 recruits other interacting transfactors or favors the DNA-binding ability of the transfactors to facilitate their transcriptional activity; however, this possibility remains to be further investigated.

ZC4H2 is a recently discovered X-linked gene that has been implicated in the regulation of the hippocampal synaptic dendrites, and its mutation leads to brain abnormalities, including intellectual disability (Hirata et al., 2013). As the LC-NA system is a well-known modulator in cognition and other high brain functions (Robertson et al., 2013), it is likely that the impaired central NA system caused by the mutation of *ZC4H2* contributes to the development of intellectual disability.

MATERIALS AND METHODS

Genotyping and maintenance of animals

All mice were maintained and handled according to guidelines approved by the Animal Committee of Fudan University and the Animal Care and Use Committee of the Kunming Institute of Zoology, Chinese Academy of Sciences. *Rnf220*, *Zc4h2* KO embryos and *Zc4h2* heterozygotes were generated as described in our previous study, and all genotypes were confirmed by PCR (Ma et al., 2019a; Ma et al., 2019b). As similar phenotypes of LC-NA neurons were found in female and male *Zc4h2* KO mice, both female and male embryos were used for analysis of phenotypes in *Zc4h2* KO mice. In the analysis of *Zc4h2* heterozygotes and their controls, only female embryos were used for related analysis.

Immunohistochemistry, BrdU labeling and *in situ* hybridization

Immunohistochemical staining and *in situ* hybridization were performed as described previously (Ma et al., 2019a; Ma et al., 2019b). Briefly, embryos were perfused with 4% paraformaldehyde and postfixed for 24 h. After cryoprotection with 20% sucrose, brains were cut into 12 µm-thick sections using a cryostat (CM1950; Leica) (Coppola et al., 2010). The following primary antibodies were used: rabbit anti-Zc4h2 (1:200; Sigma-Aldrich), rabbit anti-Phox2a (1:300; a gift from Dr A. Pattyn, French Institute of Health and Medical Research, France), rabbit anti-Phox2b (1:500; a gift from Dr A. Pattyn), mouse anti-Th (1:20,000; T1299, Sigma-Aldrich) and rabbit anti-peripherin (1:1000; ab4666, Abcam) antibodies. For double immunostaining of Th and Phox2a, Phox2b and peripherin, sections were incubated with primary antibodies at 4°C overnight, then with a mixture of biotinylated horse anti-rabbit (1:500; BA1100, Vector Laboratories) and Alexa Fluor 488-conjugated donkey anti-mouse (1:500; A21202, Invitrogen) antibodies for 3 h, and finally with Cy3-conjugated streptavidin (1:1000; 016160084, Jackson ImmunoResearch) and Hoechst 33258 (1:2000; 94403, Sigma-Aldrich) for 1 h.

For the BrdU assay, pregnant mice received one pulse of BrdU (100 mg/kg body weight; Sigma-Aldrich) by intraperitoneal injection and were euthanized 1 h later. Brain sections were sequentially subjected to citrate buffer (0.01 M, pH 6.0) at 95°C for 10 min, HCl (2 M) at 37°C for 30 min and sodium borate (0.1 M) at room temperature for 10 min. Treated sections were immunostained with rat anti-BrdU antibody (1:300; OBT0030A, Accurate Chemical & Scientific Corporation) as described above.

RNA probes for detecting *Dbh*, *Phox2a*, *Phox2b*, *Net*, *Crf*, *Aadc* and *MaoA* were generated based on Allen Brain Atlas (http://portal.brain-map.org). For *Rnf220*, probes against exon 2 (*Rnf220* E2) were generated by RT-PCR.

For double labeling of *in situ* hybridization and immunostaining, sections were treated with *in situ* hybridization procedures first. After visualization for mRNA, sections were immunostained with the required antibodies. Images were captured using an epifluorescence microscope (Eclipse 80i, Nikon).

Cell count

For quantification of Dbh^+ neurons, Dbh^+ neurons in four to six sections containing presumptive LC were counted in control and KO embryos by a trained observer who did not know the genotypes (three for each).

Plasmids, cell lines and transfection

Rnf220 and Zc4h2 constructs were described previously (Ma et al., 2019a, b). Mouse *Phox2a* and *Phox2b* open reading frame complementary DNAs were obtained by RT-PCR from E10.5 mouse embryo total RNA and then subcloned into the $pCS2^+$-N-myc expression vectors. Phox2a and Phox2b KR mutant constructs were created via a site-directed mutation with PCR-driven overlap extension, as described previously (Lim et al., 2000). HEK293 cells were cultured in DMEM containing 10% fetal bovine serum (FBS; Millipore), 100 U/ml penicillin and 100 U/ml streptomycin (Life Technologies). Mouse CATH.a cells were cultured in RPMI-1640 medium containing 8% horse serum (HS, Gibco) and 4% FBS. Both HEK293 and Cath.a cells were transfected using Lipofectamine 2000 (Invitrogen).

For knockdown of *Rnf220* and *Zc4h2* in CATH.a cells, the following siRNAs were used: si*Rnf220*-1# (siG000055182A, RiboBio), si*Rnf220*-2# (siG000055182B, RiboBio), si*Zc4h2*-1#: 5′-GGTGACCTTTCTTCCAC-AA-3′ and si*Zc4h2*-2#: 5′-GGAGGGATAGACCTCTGTT-3′.

RNA extraction, reverse transcription and real-time RT-PCR

Trizol reagent (TIANGEN) was used for total RNA extraction and reverse transcription was carried out using a First-Strand cDNA synthesis kit (Thermo Fisher Scientific). The following primers were used for real-time PCR: mouse *Rnf220* forward, 5′-TGTGGGCAGAAGCGGATAC-3′, and reverse, 5′-TGTCATCTCCATCCACATCCAG-3′; mouse *Zc4h2* forward, 5′-AGCAGGACACAAGGCAGACA-3′, and reverse, 5′-TTGCAAAGAG-GGCATATAGG-3′; mouse *Th* forward, 5′-GGGCATCCTCGATGAGA-CT-3′, and reverse, 5′-AGAAGAGCCGTCTCAGAGCA-3′; mouse *Dbh* forward, 5′-CAGCTCTGTCTGGGGGTAGT-3′, and reverse, 5′-GGGG-GACGTACTCATCACTT-3′.

Immunoprecipitation, *in vivo* ubiquitylation and western blot assays

For immunoprecipitation, HEK293 cells were lysed in IP buffer [50 mM Tris-HCL (pH 7.4), 150 mM NaCl, 5 mM EDTA (pH 8.0), and 1% Triton X-100] that contained a protease inhibitor mixture (Roche Applied Science) for 30 min on ice, and the lysates were clarified by centrifugation for 15 min at 14,000 ***g***. The protein concentration of each cell lysate sample was determined by bicinchoninic acid (BCA) assay. Immunoprecipitation was carried out with anti-FLAG M2 beads (Sigma-Aldrich). CATH.a cells and E18.5 mouse embryo brain tissues were lysed in SDS lysis buffer. Isolated proteins were subjected to SDS-PAGE followed by western blot analyses. *In vivo* ubiquitylation assays were conducted as described previously (Ma et al., 2019a). The primary antibodies used for immunoblot were: anti-myc (1:5000; C3956, Sigma-Aldrich), anti-FLAG (1:5000; F7425, Sigma-Aldrich), anti-Zc4h2 (1:1000; HPA027577, Sigma-Aldrich), anti-Phox2a (1:1000, a gift from Dr A. Pattyn), anti-Phox2b (1:1000, a gift from Dr A. Pattyn) anti-Rnf220 (1:1000; HPA049584, Sigma-Aldrich) and anti-α-tubulin (1:5000; 11224-1-AP, ProteinTech).

EMSA assays

Sense and antisense oligonucleotides corresponding to the sequences of Phox2-binding domains, containing all the three Phox2 binding domains (PBD1, PBD2 and PBD3) of the human *DBH* promoter (Seo et al., 2002) were synthesized and labeled by biotin at two ends (Sangon Biotech) with the following nucleotide sequences: forward, 5′-GTGTCATTAGTCCAA-TTAGAG-3′ and reverse, 5′-CCTCTAATTGGACTAATGACA-3′. The forward and reverse oligonucleotides were annealed, gel-purified and used as probes in EMSA. EMSA and antibody co-incubation experiments were performed according to the instructions of the EMSA kit (Thermo Fisher Scientific).

Luciferase reporter assays

To construct the human *DBH* reporter, we inserted the Phox2-binding domain including all the three Phox2 binding sites (PBD1, PBD2 and PBD3) (Seo et al., 2002) into the pGL3-Promoter vector (Promega) within MluI and XhoI sites. We verified all recombinant clones by sequencing. For luciferase reporter assays, HEK293 cells were transfected with the indicated reporter plasmids together with the same TK-*Renilla* internal control

reporter vectors by using the lipofectamine 2000 transfection reagent (Invitrogen) and given fresh medium 6 h after the transfection. Luciferase activity was measured 36 h after the transfection using the Dual-Luciferase Reporter Assay System (Promega) according to the manufacturer's instructions. All assays were performed in at least three independent experiments with a minimum of three replicates.

In ovo electroporation

In ovo electroporation was performed as described previously (Zhu et al., 2007). Fertilized chicken eggs were incubated at 38°C under humid conditions for 50 h to HH stages 12-14 and pCAG-*Phox2a*/*Phox2b*/*Rnf220*/*Zc4h2*/GFP or pCAG-*Phox2a*-KR/*Phox2b*-KR/*Rnf220*/*Zc4h2*/GFP (1 µg/µl/plasmid) were injected into the neural tube. After injection, plasmids were electroporated into the neural tube using the Electro Square Porator (ECM830; 12 V, 5 ms, 5 pulses). After 24 h, embryos were dissected out and analyzed.

Statistical analysis

All of our immunofluorescence and *in situ* hybridization assays were carried out on at least two indicated embryos. All of our western blot, EMSA, luciferase reporter and real-time RT-PCR assays were conducted at least three times. For Dbh^{+} cell count, independent-sample *t*-test was performed. For statistical analysis of *in vitro* experiments, one-way ANOVA evaluations with posthoc Student–Newman–Keuls test were performed. P values of <0.05 were considered statistically significant, and P values of <0.001 were considered statistically very significant. Graphpad Prism 8 software was used for all statistical calculations.

Acknowledgements

We thank Dr A. Pattyn for providing the Phox2a/Phox2b antibody.

Competing interests

The authors declare no competing or financial interests.

Author contributions

Conceptualization: N.-N.S., P.M., B.M., Y.-Q.D.; Methodology: N.-N.S., P.M., Q.Z.; Validation: N.-N.S., Q.Z.; Formal analysis: N.-N.S., P.M., Q.Z., Lei Zhang, Longlong Zhang, L. Zhu, C.-H.H.; Investigation: N.-N.S., P.M., Q.Z., Lei Zhang, Longlong Zhang, L. Zhu, C.-H.H., H.W.; Resources: B.M., Y.-Q.D.; Data curation: N.-N.S., P.M.; Writing - original draft: N.-N.S., P.M., B.M., Y.-Q.D.; Writing - review & editing: N.-N.S., P.M., B.M., Y.-Q.D.; Supervision: B.M., Y.-Q.D.; Project administration: B.M., Y.-Q.D.; Funding acquisition: N.-N.S., P.M., Lei Zhang, B.M., Y.-Q.D.

Funding

This project was supported by Science and Technology Commission of Shanghai Municipality Major Project (No. 2018SHZDZX01) and ZJLab, 'Strategic Priority Research Program' of the Chinese Academy of Sciences (Grant XDB13000000), the National Natural Science Foundation of China (31671061, 81571332, 31771134, 31671521, 31871483, 31500847), the National Key R&D Program of China (Ministry of Science and Technology of China, 2017YFA0104002) and Applied Basic Research Foundation of Yunnan Province (No. 2016FB043).

Supplementary information

Supplementary information available online at
http://dev.biologists.org/lookup/doi/10.1242/dev.185199.supplemental

Peer review history

The peer review history is available online at https://dev.biologists.org/lookup/doi/10.1242/dev.185199.reviewer-comments.pdf

References

Barclay, M., Noakes, P. G., Ryan, A. F., Julien, J.-P. and Housley, G. D. (2007). Neuronal expression of peripherin, a type III intermediate filament protein, in the mouse hindbrain. *Histochem. Cell Biol.* **128**, 541-550. doi:10.1007/s00418-007-0340-4

Brunet, J. F. and Pattyn, A. (2002). Phox2 genes - from patterning to connectivity. *Curr. Opin. Genet. Dev.* **12**, 435-440. doi:10.1016/S0959-437X(02)00322-2

Coppola, E., d'Autreaux, F., Rijli, F. M. and Brunet, J.-F. (2010). Ongoing roles of Phox2 homeodomain transcription factors during neuronal differentiation. *Development* **137**, 4211-4220. doi:10.1242/dev.056747

Flames, N. and Hobert, O. (2011). Transcriptional control of the terminal fate of monoaminergic neurons. *Annu. Rev. Neurosci.* **34**, 153-184. doi:10.1146/annurev-neuro-061010-113824

Haglund, K., Di Fiore, P. P. and Dikic, I. (2003). Distinct monoubiquitin signals in receptor endocytosis. *Trends Biochem. Sci.* **28**, 598-603. doi:10.1016/j.tibs.2003.09.005

Hicke, L. (2001). Protein regulation by monoubiquitin. *Nat. Rev. Mol. Cell Biol.* **2**, 195-201. doi:10.1038/35056583

Hirata, H., Nanda, I., van Riesen, A., McMichael, G., Hu, H., Hambrock, M., Papon, M. A., Fischer, U., Marouillat, S., Ding, C. et al. (2013). ZC4H2 mutations are associated with arthrogryposis multiplex congenita and intellectual disability through impairment of central and peripheral synaptic plasticity. *Am. J. Hum. Genet.* **92**, 681-695. doi:10.1016/j.ajhg.2013.03.021

Hirsch, M. R., Tiveron, M. C., Guillemot, F., Brunet, J. F. and Goridis, C. (1998). Control of noradrenergic differentiation and Phox2a expression by MASH1 in the central and peripheral nervous system. *Development* **125**, 599-608.

Holm, P. C., Rodríguez, F. J., Kele, J., Castelo-Branco, G., Kitajewski, J. and Arenas, E. (2006). BMPs, FGF8 and Wnts regulate the differentiation of locus coeruleus noradrenergic neuronal precursors. *J. Neurochem.* **99**, 343-352. doi:10.1111/j.1471-4159.2006.04039.x

Hong, S. J., Lardaro, T., Oh, M. S., Huh, Y., Ding, Y., Kang, U. J., Kirfel, J., Buettner, R. and Kim, K.-S. (2008). Regulation of the noradrenaline neurotransmitter phenotype by the transcription factor AP-2beta. *J. Biol. Chem.* **283**, 16860-16867. doi:10.1074/jbc.M709106200

Howard, M. J. (2005). Mechanisms and perspectives on differentiation of autonomic neurons. *Dev. Biol.* **277**, 271-286. doi:10.1016/j.ydbio.2004.09.034

Itoi, K. and Sugimoto, N. (2010). The brainstem noradrenergic systems in stress, anxiety and depression. *J. Neuroendocrinol.* **22**, 355-361. doi:10.1111/j.1365-2826.2010.01988.x

Kim, J., Choi, T. I., Park, S., Kim, M. H., Kim, C. H. and Lee, S. (2018). Rnf220 cooperates with Zc4h2 to specify spinal progenitor domains. *Development* **145**, dev165340. doi:10.1242/dev.165340

Kong, Q., Zeng, W., Wu, J., Hu, W., Li, C. and Mao, B. (2010). RNF220, an E3 ubiquitin ligase that targets Sin3B for ubiquitination. *Biochem. Biophys. Res. Commun.* **393**, 708-713. doi:10.1016/j.bbrc.2010.02.066

Lim, K.-C., Lakshmanan, G., Crawford, S. E., Gu, Y., Grosveld, F. and Engel, J. D. (2000). Gata3 loss leads to embryonic lethality due to noradrenaline deficiency of the sympathetic nervous system. *Nat. Genet.* **25**, 209-212. doi:10.1038/76080

Ma, P., Yang, X., Kong, Q., Li, C., Yang, S., Li, Y. and Mao, B. (2014). The ubiquitin ligase RNF220 enhances canonical Wnt signaling through USP7-mediated deubiquitination of beta-catenin. *Mol. Cell. Biol.* **34**, 4355-4366. doi:10.1128/MCB.00731-14

Ma, P., Ren, B., Yang, X., Sun, B., Liu, X., Kong, Q., Li, C. and Mao, B. (2017). ZC4H2 stabilizes Smads to enhance BMP signalling, which is involved in neural development in Xenopus. *Open Biol.* **7**, 170122. doi:10.1098/rsob.170122

Ma, P., Song, N. N., Cheng, X., Zhu, L., Zhang, Q., Zhang, L., Yang, X., Wang, H., Kong, Q., Shi, D. et al. (2019a). ZC4H2 stabilizes RNF220 to pattern ventral spinal cord through modulating Shh/Gli signaling. *J. Mol. Cell Biol.* mjz087. doi:10.1093/jmcb/mjz087

Ma, P., Song, N. N., Li, Y., Zhang, Q., Zhang, L., Zhang, L., Kong, Q., Ma, L., Yang, X., Ren, B. et al. (2019b). Fine-tuning of Shh/Gli signaling gradient by non-proteolytic ubiquitination during neural patterning. *Cell Rep* **28**, 541-553.e4. doi:10.1016/j.celrep.2019.06.017

May, M., Hwang, K.-S., Miles, J., Williams, C., Niranjan, T., Kahler, S. G., Chiurazzi, P., Steindl, K., Van Der Spek, P. J., Swagemakers, S. et al. (2015). ZC4H2, an XLID gene, is required for the generation of a specific subset of CNS interneurons. *Hum. Mol. Genet.* **24**, 4848-4861. doi:10.1093/hmg/ddv208

Morin, X., Cremer, H., Hirsch, M.-R., Kapur, R. P., Goridis, C. and Brunet, J.-F. (1997). Defects in sensory and autonomic ganglia and absence of locus coeruleus in mice deficient for the homeobox gene Phox2a. *Neuron* **18**, 411-423. doi:10.1016/S0896-6273(00)81242-8

Pattyn, A., Morin, X., Cremer, H., Goridis, C. and Brunet, J. F. (1997). Expression and interactions of the two closely related homeobox genes Phox2a and Phox2b during neurogenesis. *Development* **124**, 4065-4075.

Pattyn, A., Goridis, C. and Brunet, J.-F. (2000). Specification of the central noradrenergic phenotype by the homeobox gene Phox2b. *Mol. Cell. Neurosci.* **15**, 235-243. doi:10.1006/mcne.1999.0826

Qian, Y., Fritzsch, B., Shirasawa, S., Chen, C. L., Choi, Y. and Ma, Q. (2001). Formation of brainstem (nor)adrenergic centers and first-order relay visceral sensory neurons is dependent on homeodomain protein Rnx/Tlx3. *Genes Dev.* **15**, 2533-2545. doi:10.1101/gad.921501

Robertson, S. D., Plummer, N. W., de Marchena, J. and Jensen, P. (2013). Developmental origins of central norepinephrine neuron diversity. *Nat. Neurosci.* **16**, 1016-1023. doi:10.1038/nn.3458

Rychlik, J. L., Hsieh, M., Eiden, L. E. and Lewis, E. J. (2005). Phox2 and dHAND transcription factors select shared and unique target genes in the noradrenergic cell type. *J. Mol. Neurosci.* **27**, 281-292. doi:10.1385/JMN:27:3:281

Sara, S. J. (2009). The locus coeruleus and noradrenergic modulation of cognition. *Nat. Rev. Neurosci.* **10**, 211-223. doi:10.1038/nrn2573

Seo, H., Hong, S. J., Guo, S., Kim, H.-S., Kim, C.-H., Hwang, D.-Y., Isacson, O., Rosenthal, A. and Kim, K.-S. (2002). A direct role of the homeodomain proteins Phox2a/2b in noradrenaline neurotransmitter identity determination. *J. Neurochem.* **80**, 905-916. doi:10.1046/j.0022-3042.2002.00782.x

Shi, M., Hu, Z.-L., Zheng, M.-H., Song, N.-N., Huang, Y., Zhao, G., Han, H. and Ding, Y.-Q. (2012). Notch-Rbpj signaling is required for the development of noradrenergic neurons in the mouse locus coeruleus. *J. Cell Sci.* **125**, 4320-4332. doi:10.1242/jcs.102152

Szot, P. (2012). Common factors among Alzheimer's disease, Parkinson's disease, and epilepsy: possible role of the noradrenergic nervous system. *Epilepsia* **53** Suppl. 1, 61-66. doi:10.1111/j.1528-1167.2012.03476.x

Tilleman, H., Hakim, V., Novikov, O., Liser, K., Nashelsky, L., Di Salvio, M., Krauthammer, M., Scheffner, O., Maor, I., Mayseless, O. et al. (2010). Bmp5/7 in concert with the mid-hindbrain organizer control development of noradrenergic locus coeruleus neurons. *Mol. Cell. Neurosci.* **45**, 1-11. doi:10.1016/j.mcn.2010.05.003

Tsarovina, K., Reiff, T., Stubbusch, J., Kurek, D., Grosveld, F. G., Parlato, R., Schutz, G. and Rohrer, H. (2010). The Gata3 transcription factor is required for the survival of embryonic and adult sympathetic neurons. *J. Neurosci.* **30**, 10833-10843. doi:10.1523/JNEUROSCI.0175-10.2010

Vogel-Hopker, A. and Rohrer, H. (2002). The specification of noradrenergic locus coeruleus (LC) neurones depends on bone morphogenetic proteins (BMPs). *Development* **129**, 983-991.

Zanzottera, C., Milani, D., Alfei, E., Rizzo, A., D'Arrigo, S., Esposito, S. and Pantaleoni, C. (2017). ZC4H2 deletions can cause severe phenotype in female carriers. *Am. J. Med. Genet. A* **173**, 1358-1363. doi:10.1002/ajmg.a.38155

Zhao, G.-Y., Li, Z.-Y., Zou, H.-L., Hu, Z.-L., Song, N.-N., Zheng, M.-H., Su, C.-J. and Ding, Y.-Q. (2008). Expression of the transcription factor GATA3 in the postnatal mouse central nervous system. *Neurosci. Res.* **61**, 420-428. doi:10.1016/j.neures.2008.04.014

Zhu, X.-J., Wang, C.-Z., Dai, P.-G., Xie, Y., Song, N.-N., Liu, Y., Du, Q.-S., Mei, L., Ding, Y.-Q. and Xiong, W.-C. (2007). Myosin X regulates netrin receptors and functions in axonal path-finding. *Nat. Cell Biol.* **9**, 184-192. doi:10.1038/ncb1535